Electronic Research Archive

https://www.aimspress.com/journal/era

ERA, 34(1): 336–350.
DOI: 10.3934/era.2026016
Received: 07 November 2025
Revised: 19 December 2025
Accepted: 06 January 2026
Published: 09 January 2026

Research article

Control design of the hydraulic support pushing system based on saturation

Yuan Zhang[1], Wentao Ju[1], Qing Liu[2], Leijie Wei[1], Chunlei Yin[2], Xuejun Feng[1], Yaliang Yao[1] and Kai Chen[2,*]

[1] Shanxi Huaning Coking Coal Co., Ltd., Linfen 042102, China

[2] Beijing Tianma Intelligent Control Technology Co., Ltd., Beijing 101399, China

* **Correspondence:** Email: yincl@tdmarco.com.

Abstract: This paper focused on the control design problem regarding the hydraulic support pushing system, with full consideration of the saturation structure of the control input. With the help of the backstepping technique, some sufficient conditions were established to ensure local exponential stability of the error system between the hydraulic support pushing system and the reference system, simultaneously providing an estimation of the attractive domain. In addition, a potential relationship between the saturation structure and attractive domain was established, which was crucial for achieving local exponential stability in the framework of saturation limitations. It showed that the size of the attractive domain was not only determined by the structure of control input but was also affected by the saturation structure. Finally, some simulations were presented to illustrate the effectiveness of the proposed results.

Keywords: hydraulic support pushing system; saturation; backstepping technique; attractive domain; local exponential stability

1. Introduction

Coal is widely acknowledged as the cornerstone of energy security in China, making the assurance of safety and efficiency in coal mine production critically important. As the primary production site in coal mining, the adjustment of the hydraulic support pushing system at fully mechanized mining faces is directly linked to both coal mine safety and mining efficiency [1]. This issue has garnered significant attention, as evidenced by recent studies [2–4] and the references therein.

It is important to note that the control process of the hydraulic support pushing system often faces various challenges within the complex underground coal mine environment, particularly when attempting to achieve expected performance [5, 6]. For instance, the lack of adaptive adjustments can lead to significant deviations between the actual and predetermined trajectories. To solve these

challenges, a variety of advanced control strategies have been proposed [7–9]. Particularly, a pressure-flow coupling-based control method was provided in [7] to address the sluggish movement and poor slewing performance of traditional controls, thus improving work efficiency. Building on the radial basis function network and the dead zone model, a neural model reference adaptive disturbance rejection composite controller was proposed in [8]. This controller demonstrated improved system response characteristics, reduced steady state errors, and enhanced robustness. Moreover, [9] combined particle swarm optimization with bang-bang control to enhance stability performance and work safety by developing efficient detection and control systems.

It is important to note that the controllers designed in [7–9] are based on an idealized environment where no constraints are imposed on the control input. In reality, saturation phenomena frequently occur in the control systems. The magnitude of signals that actuators or sensors can transmit is often constrained by physical limitations and safety requirements. This is commonly observed in various industrial devices, such as hydraulic actuators [10] and electrical actuators [11]. For instance, to ensure effective out-of-step protection, the torque and rotational speed of generators must be maintained within specific limits [12]. Similarly, during horizontal maneuvering governed by an aircraft vertical stabilizer, the rudder deflection angle and movement rate are restricted in magnitude to prevent potential flight incidents [13]. It is crucial to recognize that neglecting saturation limitations during controller design can lead to adverse system performance [14]. Consequently, incorporating saturation considerations into controller design has garnered significant interest from researchers over the past few decades, as evidenced by works such as [15–18]. Generally, two classical methods address saturation limitations. The first is known as the one-step method, which integrates the saturated effect during the initial phase of controller design. In recent years, significant attention has been devoted to this method in controlling systems [19, 20]. For example, fundamental results concerning the estimation of the attractive domain for systems utilizing saturated linear feedback were presented in [19]. The other method is the anti-windup compensation technique, which essentially follows a two-step process. The first step involves ignoring the saturation limitations and designing a linear controller to meet specific performance or stability requirements. In the second step, an anti-windup compensator is introduced to mitigate the negative effects of saturation. Recently, several significant studies have addressed the phenomenon of saturation in various types of systems using this method [21–24]. For example, a novel anti-windup compensator based on a decoupled architecture was presented in [21] for constrained nonlinear time-delay systems. The design objectives of this anti-windup compensator were formulated by leveraging the reformulation capabilities of a linear parameter-varying model, which utilized the Lipschitz continuity property of the underlying nonlinearities.

On the other hand, recent research in adaptive and robust control [25, 26] has focused considerable attention on an intriguing control method known as the backstepping technique [27–30]. This technique is based on the concept of recursively selecting appropriate functions of state variables as pseudo control inputs for lower dimensional subsystems within the overall system. Each step in the backstepping process results in the formulation of a new pseudo control law, which is defined based on the laws derived in the previous stages. At the conclusion of this procedure, a feedback design for the actual control input is generated. This design achieves the original control objective through a final Lyapunov function, constructed by aggregating the Lyapunov functions corresponding to each individual design step [31–34]. However, to the best of our knowledge, the application of the

backstepping technique to address saturation limitations in hydraulic support pushing systems has received limited research attention to date, particularly regarding the establishment of the relationship between the control signal and the estimation of the attractive domain. Therefore, the fundamental and critical problem of how to design a saturated controller that enables the hydraulic support pushing system to achieve the desired performance, while also estimating the size of the attractive domain, remains unresolved and warrants thorough investigation. This issue constitutes the primary motivation for this paper.

Inspired by the above analysis, this paper focuses on the effects of saturation limitations on stability analisis and control design for the hydraulic support pushing system using the backstepping technique. The innovations of this paper mainly lie in the following aspects: first, with the help of the backstepping technique, an appropriate control design that does not account for saturation limitations will be proposed and then integrated into the saturated framework. Second, to enable the hydraulic support pushing system to achieve expected performance, a set of sufficient conditions will be derived to guarantee local exponential stability (LES) of the error system between the hydraulic support pushing system and the reference system. Third, the estimation of the attractive domain will be provided in this paper. Fourth, a potential relationship between the saturation structure and attractive domain will be established, which will show that the estimation of the attractive domain is not only dependent on the control input structure but is also influenced by the saturation structure. The remainder of this paper is organized as follows: Modeling of the hydraulic support pushing system is given in Section 2, and Section 3 presents some relevant preliminaries. Based on this, the main results, including control design and stability analysis, are proposed in Sections 4 and 5, respectively. Finally, some simulations are put forward in Section 6, and Section 7 concludes this paper.

Notations. Let $\mathbb{R}$ denote the set of real numbers, $\mathbb{R}_+$ the set of nonnegative real numbers, and $\mathbb{R}^n$ the n-dimensional real space equipped with the Euclidean norm $|\cdot|$. For two integers $n_1 < n_2$, let $\mathcal{I}[n_1, n_2] = \{n_1, n_1 + 1, \ldots, n_2\}$. Given a positive constant ρ, let $\mathcal{S}_\rho = \{x \in \mathbb{R} : |x| \leq \rho\}$.

2. Modeling of hydraulic support pushing system

2.1. Principle of the hydraulic support pushing system of the fully mechanized mining face

This paper aims to design an appropriate control input to drive the hydraulic support pushing system to achieve expected performance [35, 36]. The principle behind it is based on the interaction between the dynamic characteristic and the structural design of the hydraulic support pushing system, where the

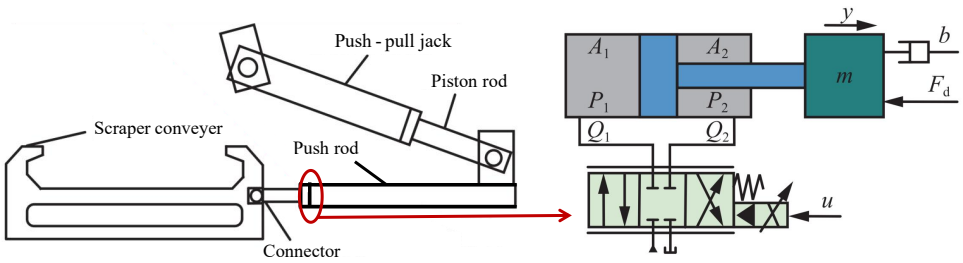

Figure 1. Hydraulic support pushing system of fully mechanized mining face.

Table 1. Parameters of hydraulic support pushing system.

Parameter	Meaning	Unit
A_1	Effective working area of the rodless chamber	m^2
A_2	Effective working area of the rod chamber	m^2
P_1	Pressure of the rodless chamber	N
P_2	Pressure of the rod chamber	N
Q_1	Flow of the rodless chamber	m^3/s
Q_2	Flow of the rod chamber	m^3/s
m	Equivalent total mass of the middle trough and coal drop	kg
y	Displacement of the piston rod	m
b	Viscous damping coefficient	$N \cdot s/m$
F_d	Integrated disturbing force	N
u	Input voltage	V

structure of which is shown in Figure 1 and the main parameters for the specification have been listed in Table 1.

One may observe from Figure 1 that the hydraulic support is adjusted through a push-pull jack, with a piston rod connected to such jack. Then with the help of the push rod, the force that is generated by input voltage will be transmitted to the connector of the middle trough for the scraper conveyor. However, due to the existence of structural clearance and flexible connection, such a process may be accompanied by response hysteresis and displacement deviation. Note that the hydraulic support pushing system is regarded as a high-inertia system in the roof support process, with a strong degree of mutual independence between adjacent supports. In contrast, it is regarded as a low-inertia system in the conveyor pushing process, where the implementation of flexible connection induces significant dynamic coupling effects. It should be pointed out that both structural hysteresis and coupling force may lead to misalignment phenomenon. This not only intensifies mutual interference between adjacent supports but also amplifies displacement deviations, ultimately affecting the control accuracy of the fully mechanized mining face.

2.2. Dynamic modeling of the hydraulic support pushing system

As is widely recognized, the key to controlling the hydraulic support pushing system lies in the precise regulation for the displacement of the piston rod (i.e., y). Such displacement is actuated by the hydraulic force exerted on the piston, of which the size is determined by the pressures of the rodless and rod chambers (i.e., P_1 and P_2). Note that the variation in such pressures is governed by the flows of the rodless and rod chambers (i.e., Q_1 and Q_2). It is worth mentioning that such flows are directly determined by the displacement of the valve spool (denoted by y_v) and the pressure differential of the valve orifice. First, the flow of the valve is formulated by

$$Q_L = K_q y_v - K_c P_L, \tag{2.1}$$

where Q_L denotes the load flow, K_q the flow gain, K_c the coefficient of flow pressure, and P_L the load pressure. Considering that the piston is in motion, the flow of the rodless chamber is given by

$Q_1 = A_1 \frac{dy}{dt}$, and that of the rod chamber is expressed as $Q_2 = A_2 \frac{dy}{dt}$. Assume that the ratio of the effective working area between the rodless and rod chambers is denoted by $N = \frac{A_1}{A_2}$. To eliminate the effect of ratio N, the flow of such two chambers is weighted and then merged as follows:

$$Q_L = \frac{Q_1 + NQ_2}{1 + N^2}. \tag{2.2}$$

Note that the variation in flow caused by oil compressibility is described by

$$\Delta Q = \frac{V_t}{2(1 + N^2)\beta_e} \cdot \frac{dP_L}{dt}, \tag{2.3}$$

where V_t is the total volume of the hydraulic cylinder and β_e is the equivalent elastic modulus of the oil. Then considering the effects of piston movement, flow, and leakage, the flow (2.2) can be rewritten as

$$Q_L = A_1 \frac{dy}{dt} + \frac{V_t}{2(1 + N^2)\beta_e} \cdot \frac{dP_L}{dt} + C_{te}P_L + C_{teo}P_S, \tag{2.4}$$

where C_{te} is the flow of external leakage, C_{teo} is the flow of internal leakage, and P_S is the oil pressure. Moreover, the force balance of the hydraulic rod is given by

$$A_1P_1 - A_2P_2 = m\ddot{y} + B_c\dot{y} + My + F_L, \tag{2.5}$$

where M is the elastic stiffness of the load; B_c is the viscous damping coefficient of the piston and load; and F_L is the load force. Based on (2.1), (2.4), and (2.5), we infer by the Laplace transformation and a simplified derivation that

$$\frac{Y}{Y_v} = \frac{\frac{K_qA_1}{K_c}\left(\frac{s^2}{\omega_h^2} + \frac{2\xi_m}{\omega_h}s + 1\right)}{\left(\frac{s}{\omega_r} + 1\right)\left(\frac{s^2}{\omega_0^2} + \frac{2\xi_0}{\omega_0}s + 1\right)}, \tag{2.6}$$

where Y is the displacement of the piston rod after the Laplace transformation; Y_v is the displacement of the valve spool after the Laplace transformation; s is the complex variable; ω_h is the mechanical natural frequency; $\xi_m = \frac{B_c}{2\sqrt{mk}}$ is the mechanical damping coefficient; $\omega_r = \frac{MK_{ce}}{A_1^2}$ is the corner frequency with the coefficient of total flow pressure K_{ce};

$$\omega_0 = A_1\sqrt{\left(1 + \frac{M}{M_h}\right) \cdot \frac{2(1 + N^2)\beta_e}{mV_t}}, \tag{2.7}$$

which is the inherent frequency with the hydraulic spring stiffness M_h; and

$$\xi_0 = \frac{K_{ce}M_h}{M_h + M}\sqrt{\frac{(1 + N^2)\beta_e m}{2V_t}} + \frac{B_c}{2A_1}\sqrt{\frac{V_t}{2(1 + N^2)\beta_e m}}, \tag{2.8}$$

which is the hydraulic and mechanical damping coefficient.

Let the state variables be defined as $(x_1, x_2, x_3)^T = (y, \dot{y}, \ddot{y})^T$. According to the above analysis and some literatures such as [2–4], Eq (2.5) can be written as follows:

$$\begin{cases} \dot{x}_1(t) = x_2(t), \\ \dot{x}_2(t) = x_3(t), \\ \dot{x}_3(t) = \omega_h[1 + \frac{K_qk}{2A_1 - A_2}]x_2(t) + \omega_h\xi_0x_3(t) + \frac{K_q\omega_h^2}{2A_1 - A_2}u(t) + E(x_1(t), x_2(t), x_3(t)), \end{cases} \tag{2.9}$$

where u is the control voltage and E is the external disturbance.

3. Preliminaries

In reality, the magnitude of the control signal generated by a controller is usually constrained by physical or safety limitations, which may lead to a fact that the actual control input is wrapped around the saturation limitation. To this end, an updated version of system (2.9) is of the form

$$\begin{cases} \dot{x}_1(t) = x_2(t), \\ \dot{x}_2(t) = x_3(t), \\ \dot{x}_3(t) = \omega_h[1 + \frac{K_q k}{2A_1 - A_2}]x_2(t) + \omega_h \xi_0 x_3(t) + \frac{K_q \omega_h^2}{2A_1 - A_2}\text{sat}_\rho(v(t)) + E(x_1(t), x_2(t), x_3(t)), \end{cases} \tag{3.1}$$

where $v \in \mathbb{R}$ is the control input without the saturation limitation and the saturated control input $\text{sat}_\rho(v) \in \mathbb{R}$ is defined by

$$\text{sat}_\rho(v) = \begin{cases} \rho, \ v \in (\rho, +\infty), \\ v, \ v \in [-\rho, \rho], \\ -\rho, \ v \in (-\infty, -\rho), \end{cases} \tag{3.2}$$

with a prior given saturation level $\rho > 0$. Consider the reference system of (3.1):

$$\begin{cases} \dot{\hat{x}}_1(t) = \hat{x}_2(t), \\ \dot{\hat{x}}_2(t) = \hat{x}_3(t), \\ \dot{\hat{x}}_3(t) = \omega_h[1 + \frac{K_q k}{2A_1 - A_2}]\hat{x}_2(t) + \omega_h \xi_0 \hat{x}_3(t) + E(\hat{x}_1(t), \hat{x}_2(t), \hat{x}_3(t)). \end{cases} \tag{3.3}$$

Let $e_i(t) = x_i(t) - \hat{x}_i(t)$, $i \in \mathcal{I}\ [1, 3]$. Then the error system is described by

$$\begin{cases} \dot{e}_1(t) = e_2(t), \\ \dot{e}_2(t) = e_3(t), \\ \dot{e}_3(t) = \omega_h[1 + \frac{K_q k}{2A_1 - A_2}]e_2(t) + \omega_h \xi_0 e_3(t) + \hat{E}(e_1(t), e_2(t), e_3(t)) + \frac{K_q \omega_h^2}{2A_1 - A_2}\text{sat}_\rho(v(t)), \end{cases} \tag{3.4}$$

where $\hat{E}(e_1, e_2, e_3) = E(x_1, x_2, x_3) - E(\hat{x}_1, \hat{x}_2, \hat{x}_3)$.

In this paper, our aim is that in the framework of the saturation limitation, the error system (3.4) can achieve stability by designing the control input v. Next, we introduce the relevant assumption and definition.

Assumption 3.1. There exist three constants $l_i \in \mathbb{R}_+$, $i \in \mathcal{I}\ [1, 3]$, such that

$$|E(s_1, s_2, s_3) - E(\hat{s}_1, \hat{s}_2, \hat{s}_3)| \le l_1|s_1 - \hat{s}_1| + l_2|s_2 - \hat{s}_2| + l_3|s_3 - \hat{s}_3|, \ s_i, \hat{s}_i \in \mathbb{R}, \ i \in \mathcal{I}\ [1, 3]. \tag{3.5}$$

Definition 3.2. Denote by $e(t) \doteq e(t, t_0, e_0)$ the solution of system (3.4) through the initial value (t_0, e_0) with $e_0 \doteq (e_1(t_0), e_2(t_0), e_3(t_0))^T \doteq (e_{10}, e_{20}, e_{30})^T \in \mathbb{R}^3$. Then system (3.4) is said to be LES with Ω, if there exist constants $M \ge 1$, $\sigma > 0$, such that for any $e_0 \in \Omega$,

$$|e(t)| \le M|e_0|e^{-\sigma(t-t_0)}, \ \forall t \ge t_0. \tag{3.6}$$

4. Control design

With the help of the backstepping technique, an appropriate control design without the saturation limitation is proposed in this section. First, the error variables are defined by

$$z_1 = e_1,\ z_2 = e_2 - \Phi_1,\ z_3 = e_3 - \Phi_2, \tag{4.1}$$

where Φ_i, $i \in \mathcal{I}\ [1, 2]$ refers to the virtual control signal, which can be designed iteratively.

Step 1. Equations (3.4) and (4.1) yield that

$$\dot{z}_1 = \dot{e}_1 = e_2 = -z_1 + e_1 + e_2. \tag{4.2}$$

Choose the Lyapunov function candidate $V_1 = \frac{1}{2}z_1^2$. Then we derive

$$\dot{V}_1 = z_1\dot{z}_1 = -z_1^2 + z_1(e_1 + e_2) = -z_1^2 + z_1z_2 + z_1(e_1 + \Phi_1). \tag{4.3}$$

It indicates that the virtual control signal can be designed by $\Phi_1 = -e_1$, implying

$$\dot{V}_1 = -z_1^2 + z_1z_2. \tag{4.4}$$

Step 2. It follows from (3.4) and (4.1) that

$$\dot{z}_2 = \dot{e}_2 - \dot{\Phi}_1 = e_3 + e_2 = -z_2 + 2e_2 + e_1 + e_3. \tag{4.5}$$

Let the Lyapunov function candidate be $V_2 = V_1 + \frac{1}{2}z_2^2$. Combined with (4.4), it derives that

$$\begin{aligned}\dot{V}_2 &= -z_1^2 + z_1z_2 + z_2\dot{z}_2\\ &= -z_1^2 - z_2^2 + z_1z_2 + z_2(2e_2 + e_1 + e_3)\\ &= -z_1^2 - z_2^2 + z_2z_3 + z_2(2e_2 + 2e_1 + \Phi_2),\end{aligned} \tag{4.6}$$

which implies that the virtual control signal can be designed by $\Phi_2 = -2e_1 - 2e_2$. Thus, we obtain

$$\dot{V}_2 = -z_1^2 - z_2^2 + z_2z_3. \tag{4.7}$$

Step 3. It can be deduced from (3.4) and (4.1) that

$$\begin{aligned}\dot{z}_3 &= \dot{e}_3 - \dot{\Phi}_2\\ &= -z_3 + \frac{K_q\omega_h^2}{2A_1 - A_2}\mathrm{sat}_\rho(v) + \left\{e_3 + \omega_h[1 + \frac{K_qk}{2A_1 - A_2}]e_2 + \omega_h\xi_0e_3 + \hat{E}(e_1, e_2, e_3) - \Phi_2 - \dot{\Phi}_2\right\}\\ &= -z_3 + \frac{K_q\omega_h^2}{2A_1 - A_2}\mathrm{sat}_\rho(v) + \Psi,\end{aligned} \tag{4.8}$$

where

$$\Psi = 2e_1 + [\omega_h(1 + \frac{K_qk}{2A_1 - A_2}) + 4]e_2 + (\omega_h\xi_0 + 3)e_3 + \hat{E}(e_1, e_2, e_3). \tag{4.9}$$

Take the Lyapunov function candidate $V_3 = V_2 + \frac{1}{2}z_3^2$. Then it follows from (4.7) that

$$\dot{V}_3 = -z_1^2 - z_2^2 + z_2 z_3 + z_3\dot{z}_3 = -z_1^2 - z_2^2 - z_3^2 + z_3\Big(\frac{K_q\omega_h^2}{2A_1 - A_2}\mathrm{sat}_\rho(v) + \Psi + e_1 + e_2\Big). \tag{4.10}$$

In the absence of the saturation limitation, the actual control input v can be designed by

$$v = -\frac{2A_1 - A_2}{K_q\omega_h^2}\Big\{3e_1 + [\omega_h(1 + \frac{K_q k}{2A_1 - A_2}) + 5]e_2 + (\omega_h\xi_0 + 3)e_3 + \hat{E}(e_1, e_2, e_3)\Big\}. \tag{4.11}$$

In this case, we infer that

$$\dot{V}_3 = -z_1^2 - z_2^2 - z_3^2 = -2V_3. \tag{4.12}$$

5. Stability analysis

In the framework of saturation limitation, some sufficient conditions are established to ensure LES for system (3.4) under control input (4.11) in this section.

Theorem 5.1. If there exist three positive constants ρ_1, ρ_2, and ρ_3, such that

$$(3 + l_1)\rho_1 + \Big\{|\omega_h[1 + \frac{K_q k}{2A_1 - A_2}] + 5| + l_2\Big\}\rho_2 + (\omega_h\xi_0 + 3 + l_3)\rho_3 \le |\frac{K_q\omega_h^2}{2A_1 - A_2}|\rho, \tag{5.1}$$

then system (3.4) is LES with

$$\mathcal{S} = \{(e_{10}, e_{20}, e_{30})^T \in \mathbb{R}^3 : e_{10} \in \mathcal{S}_{\rho_1}, e_{20} \in \mathcal{S}_{\rho_2}, e_{30} \in \mathcal{S}_{\rho_3}\} \tag{5.2}$$

under control input (4.11).

Proof. Let the Lyapunov function be $V = \frac{1}{2}z_1^2 + \frac{1}{2}z_2^2 + \frac{1}{2}z_3^2$. Then according to (4.12), it yields that $\dot{V} = -2V$. This implies that the state trajectories of e_1, e_2, and e_3 decrease to zero as t approaches infinity. Combined with (5.1) and Assumption 3.1, one infers that

$$\begin{aligned} |v(t)| &= |\frac{2A_1 - A_2}{K_q\omega_h^2}\Big\{3e_1 + [\omega_h(1 + \frac{K_q k}{2A_1 - A_2}) + 5]e_2 + (\omega_h\xi_0 + 3)e_3 + \hat{E}(e_1, e_2, e_3)\Big\}| \\ &\le |\frac{2A_1 - A_2}{K_q\omega_h^2}| \cdot |(3 + l_1)\rho_1 + \Big\{|\omega_h[1 + \frac{K_q k}{2A_1 - A_2}] + 5| + l_2\Big\}\rho_2 + (\omega_h\xi_0 + 3 + l_3)\rho_3| \\ &\le \rho, \ \forall t \ge t_0, \end{aligned} \tag{5.3}$$

i.e., $\mathrm{sat}_\rho(v(t)) \equiv v(t)$ for all $t \ge t_0$. Note that if an initial state lies outside the range $\mathcal{S}$, then (5.3) no longer holds. It indicates that the state trajectory of the considered system no longer satisfies $\dot{V} = -2V$, implying that the system may fail to achieve stability. Thus, we can conclude that system (3.4) is LES with $\mathcal{S}$ under control input (4.11). The proof is completed. □

Remark 5.2. By means of the backstepping technique, Theorem 5.1 establishes some sufficient conditions for LES of system (3.4) in the presence of saturation limitations. It is worth pointing out that when saturation is involved in system (3.1), achieving the desired performance of (3.3) via controller design requires addressing two challenging issues. To be specific, one is that the designed

controller enables system (3.4) to achieve LES in the absence of saturation. The other is that the size of the attractive domain (i.e., $\mathcal{S}$ in Theorem 5.1) should be estimated, thus ensuring that the state trajectory of system (3.4) remains within a predefined saturation bound. We address such two challenges by employing the backstepping technique and defining the saturation function with a saturated level ρ. More specifically, the designed control input (4.11) ensures the exponential convergence of system (3.4) with the help of the backstepping technique. Moreover, imposing the constraint of condition (5.1) not only ensures that the state trajectory of system (3.4) does not exceed the predefined saturation bound but also provides the estimation of attractive domain.

Remark 5.3. Note that most existing results, such as those in [2–4], focused on the control design under ideal conditions, and therefore may become invalid when the system is affected by saturation limitations. In contrast, this paper investigates the effect of saturation on the stability analysis and control design of system (3.4), and some sufficient conditions are established to ensure LES for system (3.4) with the help of the backstepping technique. In addition, Theorem 5.1 guarantees that all states of system (3.4) starting from the domain $\mathcal{S}$ remain within $\mathcal{S}$, which is crucial for the design of saturated control. As a special case of Theorem 5.1, i.e., $\hat{E}(e_1, e_2, e_3) = 0$, the following corollary can be directly obtained.

Corollary 5.4. If there exist three positive constants ρ_1, ρ_2, and ρ_3, such that

$$3\rho_1 + |\omega_h[1 + \frac{K_q k}{2A_1 - A_2}] + 5|\rho_2 + (\omega_h\xi_0 + 3)\rho_3 \leq |\frac{K_q\omega_h^2}{2A_1 - A_2}|\rho, \tag{5.4}$$

then system (3.4), with $\hat{E}(e_1, e_2, e_3) = 0$, is LES with $\mathcal{S}$ under control input

$$v = -\frac{2A_1 - A_2}{K_q\omega_h^2}\Big\{3e_1 + [\omega_h(1 + \frac{K_q k}{2A_1 - A_2}) + 5]e_2 + (\omega_h\xi_0 + 3)e_3\Big\}. \tag{5.5}$$

Table 2. Parameter values of the hydraulic support pushing system.

Parameter	Symbol	Value	Unit
Effective working area of the rodless chamber	A_1	0.0154	m^2
Effective working area of the rod chamber	A_2	0.0083	m^2
Mechanical natural frequency	ω_h	0.2	Hz
Flow gain	K_q	2	m^2/s
Coefficient of the total flow pressure	K_{ce}	0.2	m^3/s
Elastic stiffness of the load	M	40000	N/m
Hydraulic spring stiffness	M_h	30000	N/m
Equivalent elastic modulus of the oil	β_e	0.5	N/m^2
Equivalent total mass of the middle trough and coal drop	m	200	kg
Total volume of the hydraulic cylinder	V_t	0.0001	m^3
Viscous damping coefficient of the piston and load	B_c	800	$N \cdot s/m$
Mechanical damping coefficient	ξ_m	0.005	$N \cdot s/m$

6. Simulations

In this section, some simulations are put forward to illustrate the validity of our proposed theoretical result. According to the analysis of Sections 2 and 3, consider the hydraulic support pushing system as follows:

$$\begin{cases} \dot{x}_1(t) = x_2(t), \\ \dot{x}_2(t) = x_3(t), \\ \dot{x}_3(t) = \omega_h[1 + \frac{K_q k}{2A_1 - A_2}]x_2(t) + \omega_h \xi_0 x_3(t) + \frac{K_q \omega_h^2}{2A_1 - A_2}\text{sat}_\rho(v(t)) + E(x_1(t), x_2(t), x_3(t)). \end{cases} \tag{6.1}$$

Let the reference system of (6.1) be the form of

$$\begin{cases} \dot{\hat{x}}_1(t) = \hat{x}_2(t), \\ \dot{\hat{x}}_2(t) = \hat{x}_3(t), \\ \dot{\hat{x}}_3(t) = \omega_h[1 + \frac{K_q k}{2A_1 - A_2}]\hat{x}_2(t) + \omega_h \xi_0 \hat{x}_3(t) + E(\hat{x}_1(t), \hat{x}_2(t), \hat{x}_3(t)). \end{cases} \tag{6.2}$$

Let $e_i(t) = x_i(t) - \hat{x}_i(t)$, $i \in \mathcal{I}\,[1, 3]$. Then the error system is described by

$$\begin{cases} \dot{e}_1(t) = e_2(t), \\ \dot{e}_2(t) = e_3(t), \\ \dot{e}_3(t) = \omega_h[1 + \frac{K_q k}{2A_1 - A_2}]e_2(t) + \omega_h \xi_0 e_3(t) + \hat{E}(e_1(t), e_2(t), e_3(t)) + \frac{K_q \omega_h^2}{2A_1 - A_2}\text{sat}_\rho(v(t)), \end{cases} \tag{6.3}$$

where the main parameters are listed in Table 2 and the corresponding physical basis and sources can be found in [2–4]. Moreover,

$$E(x_1, x_2, x_3) = 3\sin(x_1) + 10\sin(x_2) + 4\sin(x_3) - 711120x_2 - 25.6x_3, \tag{6.4}$$

which implies that

$$\hat{E}(e_1, e_2, e_3) = 3(\sin(x_1) - \sin(\hat{x}_1)) + 10(\sin(x_2) - \sin(\hat{x}_2)) + 4(\sin(x_3) - \sin(\hat{x}_3)) - 711120e_2 - 25.6e_3. \tag{6.5}$$

Our objective is to design an appropriate controller that enables system (6.3) to achieve stability. To this end, we design the control input of the form

$$v = -\frac{9}{32}\Big\{3e_1 + \frac{32000234}{45}e_2 + (\frac{120\sqrt{30605}}{7\sqrt{13778}} + \frac{332}{77\sqrt{61210}} + 3)e_3 + \hat{E}(e_1, e_2, e_3)\Big\}. \tag{6.6}$$

Then it follows from Theorem 5.1 that system (6.3) is LES with

$$\mathcal{S} = \{(e_{10}, e_{20}, e_{30})^T \in \mathbb{R}^3 : e_{10} \in \mathcal{S}_{\rho_1}, e_{20} \in \mathcal{S}_{\rho_2}, e_{30} \in \mathcal{S}_{\rho_3}\} \tag{6.7}$$

under the control input of the form (6.6), where three positive constants ρ_1, ρ_2, and ρ_3 satisfy

$$6\rho_1 + \frac{64001084}{45}\rho_2 + (\frac{120\sqrt{30605}}{7\sqrt{13778}} + \frac{332}{77\sqrt{61210}} + 32.6)\rho_3 \le \frac{32}{9}\rho. \tag{6.8}$$

Especially, by using MATLAB tool-box, let $\rho_1 = 0.1$, $\rho_2 = 0.0001$, $\rho_3 = 0.1$, and $\rho = 81$, satisfying stability condition (6.8). Under the step size 0.00001, the state trajectories of system (6.3) have shown in Figure 2, with initial states $e_{10} = 0.1$, $e_{20} = 0.0001$, and $e_{30} = 0.1$. In addition, the state trajectories of hydraulic support pushing system (6.1) and reference system (6.2) are depicted in Figure 3, which illustrates that control input (6.6) can drive the hydraulic support pushing system to achieve expected performance. Interestingly, if the saturation constraint is not considered during controller design, the magnitude of the initial value remains unconstrained. One may observe from Figure 4 that the error system fails to achieve stability, indicating that the hydraulic support pushing system cannot attain a desired performance.

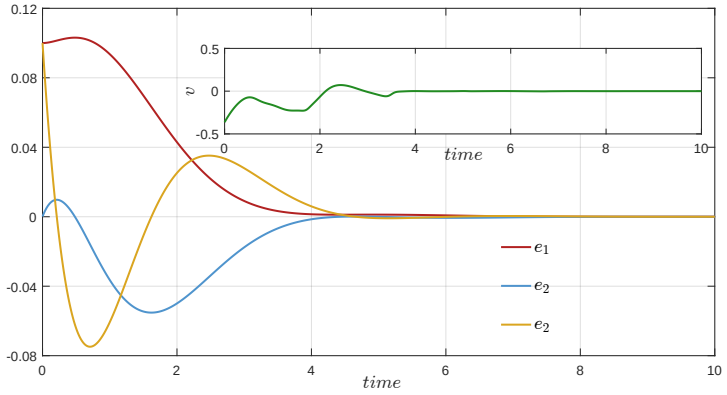

Figure 2. The state trajectories of system (6.3).

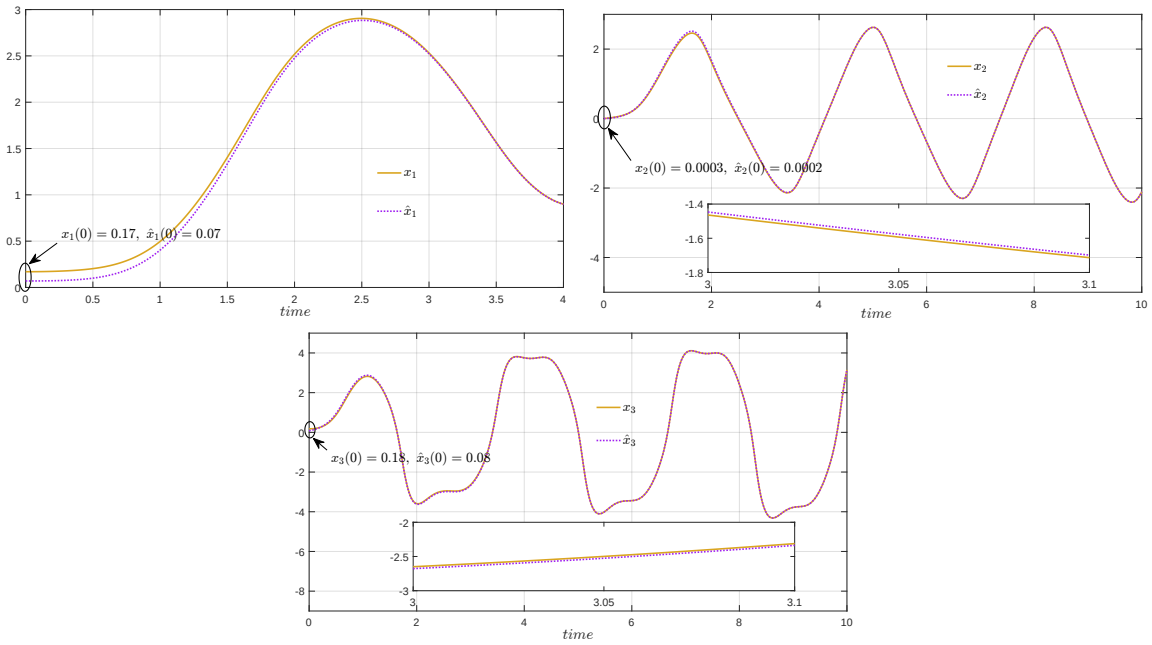

Figure 3. The state trajectories of system (6.1) and system (6.2).

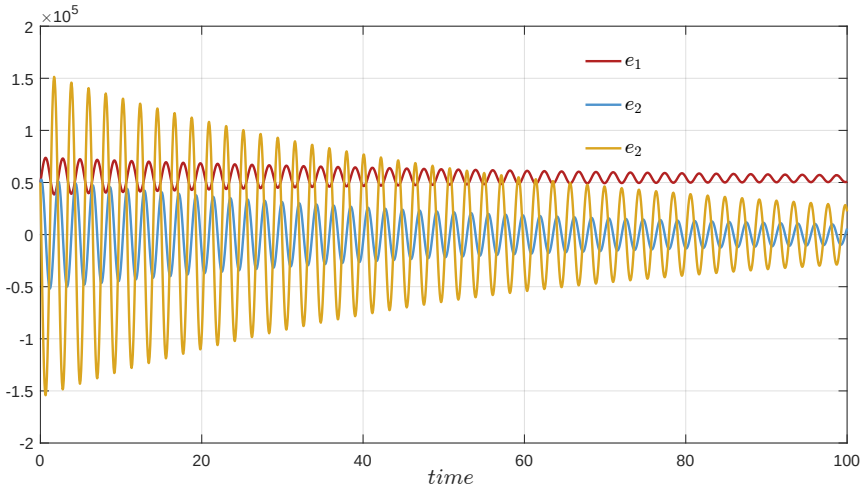

Figure 4. The state trajectories of system (6.3) without taking saturation into account.

7. Conclusions

This paper investigates the effect of saturation on the stability analysis and control design regarding the hydraulic support pushing system. To drive the hydraulic support pushing system toward achieving the desired performance, an appropriate control input is designed with the help of the backstepping technique. In addition, some sufficient conditions are established to ensure LES of the error system between the hydraulic support pushing system and the reference system, simultaneously providing an estimation of the attractive domain. Finally, some simulations are presented to verify the validity of the proposed result. Future work will focus on further exploration of saturated control methods. One of our possible research topics in the near future is to extend the result proposed in this paper to the saturated delay impulsive control problem for the hydraulic support pushing system. However, in many practical applications, the information regarding time delays in impulses is unmeasurable. Therefore, another interesting topic is the development of the hydraulic support pushing system with unmeasurable impulsive delays.

Use of AI tools declaration

The authors declare they have not used Artificial Intelligence (AI) tools in the creation of this article.

Acknowledgments

This work was supported by National Key R & D Program of China (2023YFC2907504).

Conflict of interest

The authors declare there are no conflicts of interest.

References

1. G. Wang, H. Ren, G. Zhao, S. Gong, Y. Du, Z. Xue, et al., Digital model and giant system coupling technology system of smart coal mine, *J. China Coal Soc.*, **47** (2022), 61–74.
2. Z. Zhang, Y. Liu, L. Bo, Y. Wang, Enhanced path tracking control of hydraulic support pushing mechanism via adaptive sliding mode technique in coal mine backfill operations, *Heliyon*, **10** (2024).
3. V. Milić, Ž. Šitum, M. Essert, Robust hosition position control synthesis of an electro-hydraulic servo system, *ISA Trans.*, **49** (2010), 535–542. https://doi.org/10.1016/j.isatra.2010.06.004
4. T. Hou, C. Shi, Z. Kou, J. Wu, B. Zhang, Y. Peng, Research on positioning control strategy of hydraulic support pushing system based on multistage speed control valve, *Sci. Rep.*, **14** (2024), 19046. https://doi.org/10.1038/s41598-024-70087-1
5. S. Shanmugam, R. Vadivel, S. Sabarathinam, P. Hammachukiattikul, N. Gunasekaran, Enhancing synchronization criteria for fractional-order chaotic neural networks via intermittent control: An extended dissipativity approach, *Math. Modell. Control*, **5** (2025), 31–47. https://doi.org/10.3934/mmc.2025003
6. Y. Wang, K. Li, Exponential synchronization of fractional order fuzzy memristor neural networks with time-varying delays and impulses, *Math. Modell. Control*, **5** (2025), 164–179. https://doi.org/10.3934/mmc.2025012
7. R. Zhou, L. Meng, X. Yuan, Z. Qiao, Research and experimental analysis of hydraulic cylinder position control mechanism based on pressure detection, *Machines*, **10** (2021), 1. https://doi.org/10.3390/machines10010001
8. S. Jiang, H. Wang, G. Zhao, Research on neural network model reference adaptive disturbance rejection control of digital hydraulic cylinder, *Adv. Mech. Eng.*, **14** (2022), 16878132221140706. https://doi.org/10.1177/16878132221140706
9. Y. Zhang, H. Zhang, K. Gao, Q. Zeng, F. Meng, J. Cheng, Research on intelligent control system of hydraulic support based on position and posture detection, *Machines*, **11** (2022), 33. https://doi.org/10.3390/machines11010033
10. C. Wang, X. Ji, Z. Zhang, B. Zhao, L. Quan, A. Plummer, Tracking differentiator based back-stepping control for valve-controlled hydraulic actuator system, *ISA Trans.*, **119** (2022), 208–220. https://doi.org/10.1016/j.isatra.2021.02.028
11. R. Yang, M. Queiroz, M. Li, Neural network-based control of neuromuscular electrical stimulation with input saturation, *IFAC-PapersOnLine*, **51** (2019), 170–175. https://doi.org/10.1016/j.ifacol.2019.01.061
12. E. Farantatos, R. Huang, G. Cokkinides, A. Meliopoulos, A predictive generator out-of-step protection and transient stability monitoring scheme enabled by a distributed dynamic state estimator, *IEEE Trans. Power Delivery*, **31** (2015), 1826–1835. https://doi.org/10.1109/TPWRD.2015.2512268
13. O. Brieger, M. Kerr, D. Leißling, I. Postlethwaite, J. Sofrony, M. Turner, Flight testing of a rate saturation compensation scheme on the ATTAS aircraft, *Aerosp. Sci. Technol.*, **13** (2009), 92–104. https://doi.org/10.1016/j.ast.2008.05.003

14. G. Stein, Respect the unstable, *IEEE Control Syst. Mag.*, **23** (2003), 12–25. https://doi.org/10.1109/MCS.2003.1213600

15. S. Wu, X. Li, Finite-time stabilization of nonlinear systems with actuator saturation, *IEEE Trans. Autom. Sci. Eng.*, **22** (2024), 7582–7589. https://doi.org/10.1109/TASE.2024.3466049

16. X. Li, C. Zhu, Saturated impulsive control of nonlinear systems with applications, *Automatica*, **142** (2022), 110375. https://doi.org/10.1016/j.automatica.2022.110375

17. K. Dehingia, A. Das, E. Hincal, K. Hosseini, S. Din, Within-host delay differential model for SARS-CoV-2 kinetics with saturated antiviral responses, *Electron. Res. Arch.*, **20** (2023), 20025–20049. https://doi.org/10.3934/mbe.2023887

18. K. Gao, Global boundedness of classical solutions to a Keller-Segel-Navier-Stokes system involving saturated sensitivity and indirect signal production in two dimensions, *Electron. Res. Arch.*, **20** (2023), 1710–1736. https://doi.org/10.3934/era.2023089

19. T. Hu, Z. Lin, B. Chen, An analysis and design method for linear systems subject to actuator saturation and disturbance, *Automatica*, **38** (2002), 351–359. https://doi.org/10.1016/S0005-1098(01)00209-6

20. X. Lin, S. Li, Y. Zou, Finite-time stabilization of switched linear time-delay systems with saturating actuators, *Appl. Math. Comput.*, **299** (2017), 66–79. https://doi.org/10.1016/j.amc.2016.11.039

21. A. Akram, M. Hussain, N. Saqib, M. Rehan, Dynamic anti-windup compensation of nonlinear time-delay systems using LPV approach, *Nonlinear Dyn.*, **90** (2017), 513–533. https://doi.org/10.1007/s11071-017-3678-8

22. M. Hussain, M. Rehan, C. Ahn, K. Hong, N. Saqib, Simultaneous design of AWC and nonlinear controller for uncertain nonlinear systems under input saturation, *Int. J. Robust Nonlinear Control*, **29** (2019), 2877–2897. https://doi.org/10.1002/rnc.4529

23. A. Rehman, M. Rehan, M. Riaz, M. Abid, N. Iqbal, Consensus tracking of nonlinear multi-agent systems under input saturation with applications: A sector-based approach, *ISA Trans.*, **107** (2020), 194–205. https://doi.org/10.1016/j.isatra.2020.07.030

24. M. Razaq, M. Rehan, M. Tufail, C. Ahn, Multiple Lyapunov functions approach for consensus of one-sided Lipschitz multi-agents over switching topologies and input saturation, *IEEE Trans. Circuits Syst. II Express Briefs*, **67** (2020), 3267–3271. https://doi.org/10.1109/TCSII.2020.2986009

25. N. Kumar, K. Chaudhary, Position tracking control of nonholonomic mobile robots via H infty-based adaptive fractional-order sliding mode controller, *Math. Modell. Control*, **5** (2025), 121–130. https://doi.org/10.3934/mmc.2025009

26. L. Zhou, J. Hu, B. Li, Partial-nodes-based state estimation for complex networks under hybrid attacks: A dynamic event-triggered approach, *Math. Modell. Control*, **5** (2025), 202–215. https://doi.org/10.3934/mmc.2025015

27. M. Krstic, P. Kokotovic, I. Kanellakopoulos, *Nonlinear and Adaptive Control Design*, John Wiley & Sons, Inc., 1995.

28. I. Kanellakopoulos, P. Kokotovic, A. Morse, Systematic design of adaptive controllers for feedback linearizable systems, in *1991 American Control Conference*, (1991), 649–654. https://doi.org/10.23919/ACC.1991.4791451

29. P. Kokotovic, The joy of feedback: Nonlinear and adaptive, *IEEE Control Syst. Mag.*, **12** (1992), 7–17. https://doi.org/10.1109/37.165507

30. Y. Sun, M. Zhu, Y. Zhang, T. Chen, Adaptive incremental backstepping control of stratospheric airships using time-delay estimation, *Electron. Res. Arch.*, **33** (2025), 2925–2946. https://doi.org/10.3934/era.2025128

31. M. Krstić, I. Kanellakopoulos, P. Kokotović, Adaptive nonlinear control without overparametrization, *Syst. Control Lett.*, **19** (1992), 177–185. https://doi.org/10.1016/0167-6911(92)90111-5

32. M. Krstic, P. Kokotovic, Adaptive nonlinear design with controller-identifier separation and swapping, *IEEE Trans. Autom. Control*, **40** (1995), 426–440. https://doi.org/10.1109/9.376055

33. C. Kwan, F. Lewis, Robust backstepping control of nonlinear systems using neural networks, *IEEE Trans. Syst. Man Cybern Part A Syst. Hum.*, **30** (2002), 753–766. https://doi.org/10.1109/3468.895898

34. Y. Zhang, P. Peng, Z. Jiang, Stable neural controller design for unknown nonlinear systems using backstepping, *IEEE Trans. Neural Networks*, **11** (2000), 1347–1360. https://doi.org/10.1109/72.883443

35. W. Zhou, K. Wang, W. Zhu, Synchronization for discrete coupled fuzzy neural networks with uncertain information via observer-based impulsive control, *Mathe. Modell. Control*, **4** (2024), 17–31. https://doi.org/10.3934/mmc.2024003

36. X. Zheng, J. Wang, K. Shi, Y. Tang, J. Cao, Novel stability criterion for DNNs via improved asymmetric LKF, *Math. Modell. Control*, **4** (2024), 307–315. https://doi.org/10.3934/mmc.2024025

AIMS Press